Signal transducer of inflammation gp130 modulates atherosclerosis in mice and man

Maren Luchtefeld,[1] Heribert Schunkert,[2] Monika Stoll,[3] Tina Selle,[1] Rachel Lorier,[4] Karsten Grote,[1] Christian Sagebiel,[1] Kumaravelu Jagavelu,[1] Uwe J.F. Tietge,[5] Ulrike Assmus,[6] Konrad Streetz,[6] Christian Hengstenberg,[7] Marcus Fischer,[7] Björn Mayer,[2] Karen Maresso,[4] Nour Eddine El Mokhtari,[8] Stefan Schreiber,[8] Werner Müller,[9] Udo Bavendiek,[1] Christina Grothusen,[1] Helmut Drexler,[1] Christian Trautwein,[6] Ulrich Broeckel,[4] and Bernhard Schieffer[1]

[1]Abteilung für Kardiologie und Angiologie, Medizinische Hochschule Hannover, 30625 Hannover, Germany
[2]Medizinische Klinik II, Universitätsklinikum Schleswig-Holstein, 23562 Lübeck, Germany
[3]Genetische Epidemiologie vaskulärer Erkrankungen, Leibniz-Institute for Arteriosclerosis Research, Univerity of Münster, 48149 Münster, Germany
[4]Human and Molecular Genetics Center, Medical College of Wisconsin, Milwaukee, WI 53226
[5]Center for Liver, Digestive and Metabolic Diseases, University Medical Center Groningen, 9713 GZ Groningen, Netherlands
[6]Medizinische Klinik III, RWTH Aachen, 52062 Aachen, Germany
[7]Klinik und Poliklinik für Innere Medizin II, Klinikum der Universität Regensburg, 93053 Regensburg, Germany
[8]Department of Cardiology, Institute for Clinical Molecular Biology and Department of General Medicine, Christian Albrecht University, D-2300 Kiel, Germany
[9]Department of Experimental Immunology, Gesellschaft für Biotechnologische Forschung, D-38124 Braunschweig, Germany

Liver-derived acute phase proteins (APPs) emerged as powerful predictors of cardiovascular disease and cardiovascular events, but their functional role in atherosclerosis remains enigmatic. We report that the gp130 receptor, which is a key component of the inflammatory signaling pathway within hepatocytes, influences the risk of atherosclerosis in a hepatocyte-specific gp130 knockout. Mice on an atherosclerosis-prone genetic background exhibit less aortic atherosclerosis ($P < 0.05$) with decreased plaque macrophages ($P < 0.01$). Translating these findings into humans, we show that genetic variation within the human gp130 homologue, interleukin 6 signal transducer (IL6ST), is significantly associated with coronary artery disease (CAD; $P < 0.05$). We further show a significant association of atherosclerotic disease at the ostium of the coronary arteries ($P < 0.005$) as a clinically important and heritable subphenotype in a large sample of families with myocardial infarction (MI) and a second independent population–based cohort. Our results reveal a central role of a hepatocyte-specific, gp130-dependent acute phase reaction for plaque development in a murine model of atherosclerosis, and further implicate IL6ST as a genetic susceptibility factor for CAD and MI in humans. Thus, the acute phase reaction should be considered an important target for future drug development in the management of CAD.

CORRESPONDENCE
Bernhard Schieffer:
Schieffer.Bernhard@MH-Hannover.de

Abbreviations used: APP, acute phase protein; APR, acute phase response; BMI, body mass index; CAD, coronary artery disease; CNTF, ciliary neurotrophic factor; CT, cardiotrophin; HDL, high-density lipoprotein; IL6ST, IL 6 signal transducer; LIF, leukemia inhibitory factor; MAPK, mitogen-activated protein kinase; MASMC, mouse aortic SMC; MI, myocardial infarction; OR, odds ratio; OSM, oncostatin M; SAA, serum amyloid A; SMC, smooth muscle cell; SNP, single-nucleotide polymorphism; STAT, signal transducer and activator of transcription; TC, total cholesterol.

Atherosclerosis is a chronic inflammatory disease and one of the major causes of death worldwide (1). The traditional pathophysiological paradigm of atherosclerosis includes proinflammatory mediators such as IL-6 family cytokines (2, 3), which stimulate an acute phase response (APR) via their hepatocyte gp130 receptor component. Acute phase proteins, e.g., C-reactive protein, serum amyloid A (SAA), and most likely others, are strong and consistent inflammatory markers that are associated with cardiovascular events, i.e., myocardial infarction (MI), stroke, peripheral artery disease, and sudden cardiac death in healthy individuals, as well as in patients with acute coronary syndromes (4, 5). The IL-6 cytokine family includes IL-6, IL-11, leukemia inhibitory factor (LIF), oncostatin M (OSM), ciliary neurotrophic factor (CNTF), and cardiotrophin-1 (CT-1), which share the signal transducer gp130 in their receptors. After receptor–ligand binding,

U. Broeckel and B. Schieffer contributed equally to this paper.
W. Müller's present address is Faculty of Life Sciences, University of Manchester, Manchester, UK, M13 9PT.
The online version of this article contains supplemental material.

dimerization of gp130 occurs, which activates intracellular signaling cascades, such as the JAK–signal transducer and activator of transcription (STAT) pathway and the SH2-containing tyrosine phosphatase 2 (SHP2)–RAS–mitogen-activated protein kinase (MAPK) pathway, via tyrosine phosphorylation. Activated JAKs phosphorylate tyrosine residues in the cytoplasmatic tail of gp130, providing docking sites for the SH2 domain of STAT1, STAT3, and SHP2, which are subsequently phosphorylated by JAKs. SHP2 is an adaptor that links tyrosine-phosphorylated receptors and the activation of the RAS–MAP kinase signaling pathway (6, 7). Moreover, Schaper et al. demonstrated that activation of SHP2 via gp130 requires tyrosine kinase Jak1 and limits acute-phase protein expression (8).

Upon gp130 activation, various APPs are produced within hepatocytes; in humans, mainly CRP and SAA, fibrinogen, haptoglobin, and angiotensinogen are produced. In mice, SAA represents the predominant APP, whereas CRP is a minor APP, potentially caused by the limited responsiveness of the gene to inflammatory cytokine signals (9). The transient APR is the immediate set of inflammatory reactions that is thought to serve as a first-line response of unspecific immune defence to counteract tissue injury and bacterial or fungal infections. CRP and SAA are nonspecific, but sensitive, markers of infection and tissue inflammation; they also possess intrinsic biological properties, such as activating the complement cascade, mediating phagocytosis, and regulating the inflammatory response (10). Interestingly, patients with a chronically activated inflammatory response, e.g., those with rheumatoid arthritis or lupus erythematosus, have an increased risk of atherosclerotic cardiovascular events, suggesting that the persistence of the APR over a prolonged period of time may have detrimental cardiovascular consequences. We further investigate the role of gp130 in regard to functional mechanisms related to the development of CAD. We demonstrate that a hepatocyte-specific knockout mouse for gp130 on an atherosclerosis-prone background exhibits less aortic atherosclerosis, which is concomitant with a decrease of macrophages in the lesions. Translating the functional evidence from the animal model to humans, genetic association studies can evaluate whether a gene and genetic variation in a candidate gene contributes significantly to the disease process. Genetic association analysis in two independent populations show consistent evidence for association, supporting the notion that gp130 influences the risk of atherosclerosis in humans. The combined evidence from both animals and humans provides a functional mechanism of action in the animal model and suggests that gp130 plays an important role in the atherosclerotic disease process in humans.

RESULTS

Hepatocyte-specific gp130 knockout influences atherosclerosis

Transgenic mice expressing the Cre recombinase (Cre) under the control of the hepatocyte-specific albumin promoter (11) were crossed with animals carrying the gp130 gene with loxP sites flanking exon 16, coding for the gp130 transmembrane domain (12). For this animal model, it was recently reported that a >90% deletion of exon 16 could be observed in the liver of adult mice (13). In these mice, the induction of an APR is strongly impaired (13). To define the role of the

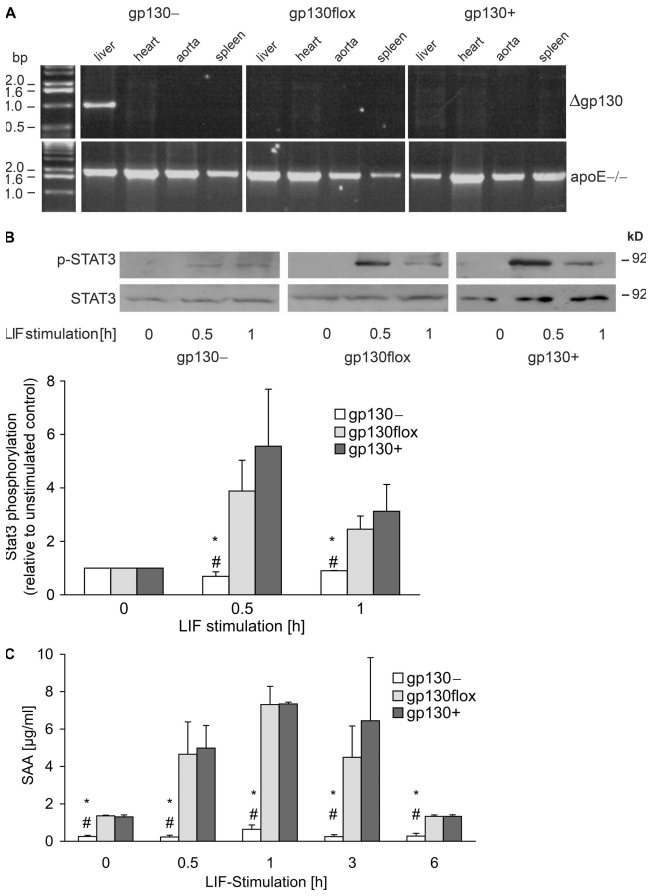

Figure 1. Analysis of murine hepatocyte-specific gp130 knockout. (A) Confirmation of gp130 deletion specifically in the liver by PCR. The forward primer anneals in exon 15 and the reverse primer anneals in exon 17. Cre-mediated excision of the lox-flanked exon 16 leads to an amplified PCR-fragment of 1,000 bp. Genotyping of all samples for apoE deficiency was performed as a positive control for DNA amplification. (B) Isolated hepatocytes of all three genotypes after stimulation with 50 ng/ml of the IL-6 cytokine LIF. The Western blot of cellular protein shows strong STAT3 tyrosine phosphorylation in the case of the controls with intact gp130, but only a weak signal in the case of gp130– hepatocytes. STAT3 served as loading control. Intensities of phosphorylated STAT3 and total STAT3 were quantified, and fold induction was calculated relative to unstimulated controls (mean ± the SEM; $n = 4$; *, $P < 0.05$ vs. gp 130+; #, $P < 0.05$ vs. gpflox). (C) SAA concentration in the supernatant of LIF-stimulated hepatocytes. Under control conditions, 0.25 ± 0.1 µg/ml SAA were measured in the supernatant of LIF-stimulated gp130–-derived hepatocytes in comparison to 1.4 ± 0.04 µg/ml SAA, which is released from gp130flox-derived hepatocytes and 1.3 ± 0.1 µg/ml SAA, which is released from gp130+-derived hepatocytes. SAA release peaks after 1 h of LIF stimulation (0.64 ± 0.24 µg/ml from gp130–-derived hepatocytes, 7.3 ± 0.97 µg/ml from gp130flox-derived hepatocytes, and 7.4 ± 0.1 µg/ml SAA from gp130+-derived hepatocytes; mean± the SD; $n = 5$; *, $P < 0.05$ vs. gp130flox; #, $P < 0.05$ vs. gp130+).

liver-derived APR in atherosclerosis, these genetic variations were transferred onto a background susceptible for this disease, *apoE*$^{-/-}$ mice. For identification of the different genotypes, the following abbreviations are used: gp130– for *cre*^{tg};*gp130*$^{flox/flox}$;*apoE*$^{-/-}$, gp130flox for *gp130*$^{flox/flox}$;*apoE*$^{-/-}$ (control), and gp130+ for *gp130*$^{+/+}$;*apoE*$^{-/-}$ (control). Phenotypically, the mice showed no significant differences. Moreover, pilot studies without cholesterol feeding revealed neither increased mortality nor increased number of infectious diseases in all three mice strains. To verify that the genetic modifications were successful, as expected, the specificity of the Cre-mediated deletion, as well as the absence of the APR, was confirmed (Fig. 1). Using a PCR reaction specific for the deletion, we demonstrate gene inactivation exclusively in liver, but not in heart, aorta, or spleen (Fig. 1 A). Using isolated hepatocytes, we confirmed that after stimulation with LIF, which is a member of the IL-6 family, induction of STAT3 phosphorylation (Fig. 1 B) and the APR as determined by SAA production (Fig. 1 C) are greatly reduced in gp130– mice, but strongly increased in the controls.

Next, we analyzed the impact of hepatocyte-specific gp130 deletion on atherosclerosis in 10-wk-old male mice after feeding with a high-fat, Western-type diet for 8 and 12 wk. Mice were assessed for aortic plaque formation by en face preparation after oil red O staining. Additionally, total lesion size was analyzed in aortic root sections after oil red O staining (Fig. 2 A, right). The quantification revealed that the atherosclerotic plaque area was reduced by >50% ($P < 0.05$) after 8 wk of feeding and 50% ($P < 0.03$) after 12 wk of feeding in aortas and aortic roots of gp130– mice (oil red O–positive area: 2.5 ± 1.9% after 8 wk and 6.2 ± 2.3% after 12 wk, compared with gp130flox [6.2 ± 0.5% after 8 wk and 13.2 ± 4.8% after 12 wk] and gp130+ mice [6.4 ± 2.8% after 8 wk and 13.4 ± 2.7% after 12 wk]; total lesion area: 0.05 ± 0.06 after 8 wk and 0.34 ± 0.11 after 12 wk compared with gp130flox [0.46 ± 0.17 after 8 wk and 0.58 ± 0.09 after 12 wk] and gp130+ [0.47 ± 0.14 after 8 wk and 0.51 ± 0.09 after 12 wk]; Fig. 2 B). Because the in vitro and in vivo experiments revealed no phenotypic differences between the gp130flox and gp130+ control groups, further analyses were performed on gp130− animals using gp130flox as control.

Markers of inflammation in gp130 knockout

Next, we investigated whether feeding with a high-fat, Western-type diet affects plasma SAA levels in these mice. We observed significantly lower SAA levels in the plasma of gp130− mice compared with gp130flox (Fig. 2 C), whereas plasma total cholesterol (TC) levels were not different between the experimental groups (Table I).

Because macrophage recruitment to the vessel wall and foam cell formation are hallmarks of atherosclerotic plaque development, we delineated the role of an APR on macrophage recruitment into aortic plaques by immunohistochemistry using monocytes/macrophages staining (MOMA-2 antisera; Fig. 2 D). The quantitative analysis revealed a significant reduction of macrophage-positive plaque area ($P < 0.01$) in gp130− (22.6 ± 3.9%) versus gp130flox (33.8 ± 2.2%) animals (Fig. 2 E). Corresponding to this finding, we observed a reduced mRNA expression of macrophage chemoattractant protein-1 (CCL2, formerly known as MCP-1) in aortic tissue of gp130− mice (Fig. 2 F) and significantly less circulating CCL2 protein in the plasma of gp130− mice (Fig. 2 G).

Table I. Plasma lipids of Western diet–treated mice

milligrams/deciliter	gp130–	gp130flox
TC	828 ± 98	705 ± 70
triglycerides	147 ± 36	146 ± 31
VLDL cholesterol	437 ± 68	385 ± 51
LDL cholesterol	299 ± 31	264 ± 20
HDL cholesterol	56 ± 4	56 ± 3

Plasma TC levels after 12 wk of Western diet are not significantly different between the experimental groups (mean ± SEM; $n = 7$).

Because CCL2 expression is required for monocyte/macrophage recruitment into the vessel wall, we determined CCL2 in isolated mouse aortic smooth muscle cells (MASMCs) after SAA stimulation. A dose–response curve for SAA revealed a significant release of CCL2 at a SAA concentration of 25 μg/ml, which further increased at a SAA concentration of 50 μg/ml (Fig. 3 A). CCL2 mRNA expression was already increased at 1 h, followed by a marked release of the protein into the supernatant after 3 h (Fig. 3, B and C). Subsequently, we tested supernatants from stimulated hepatocytes isolated from our different mouse genotypes (gp130– and gp130flox) for their ability to induce CCL2 release from MASMCs isolated from wild-type mice (C57BL/6). CCL2 release from MASMCs was enhanced when stimulated with supernatant from gp130flox hepatocytes, and was significantly reduced when stimulated with supernatant from gp130– hepatocytes (Fig. 3 D). To investigate whether SAA is the APP responsible for macrophage migration, we stimulated macrophages with the supernatant from gp130flox hepatocytes pretreated with a SAA antibody and compared the migratory efficiency with macrophages stimulated with the supernatant from gp130flox hepatocytes pretreated with an unspecific IgG. We observed a reduced migration when stimulated with the SAA-pretreated supernatant (54.5 ± 10.5% migration with SAA-AB–treated supernatant, compared with 100 ± 16.6% migration with IgG-treated supernatant; *, $P < 0.05$ vs. IgG-pretreated supernatant), pointing to an SAA-dependent migration of macrophages in murine atherosclerosis. To identify further proteins that are potentially involved in macrophage migration, a mouse cytokine protein array from SAA-stimulated (25 μg/ml for 3 h) smooth muscle cells (SMCs) was performed. Array analysis is summarized in Fig. S1 (available at http://www.jem.org/cgi/content/full/jem.20070120/DC1). Chemokines such as keratinocyte-derived chemokine (4.4 ± 0.8-fold), macrophage inflammatory protein 2 (1.5 ± 0.1-fold), and CCL2 (2.1 ± 0.2-fold) are significantly increased upon SAA stimulation, whereas proinflammatory cytokines, such as IL-6 (1.0 ± 0.2-fold) and IL-1β (1.2 ± 0.1-fold), remained unchanged compared with the unstimulated control. CCL2

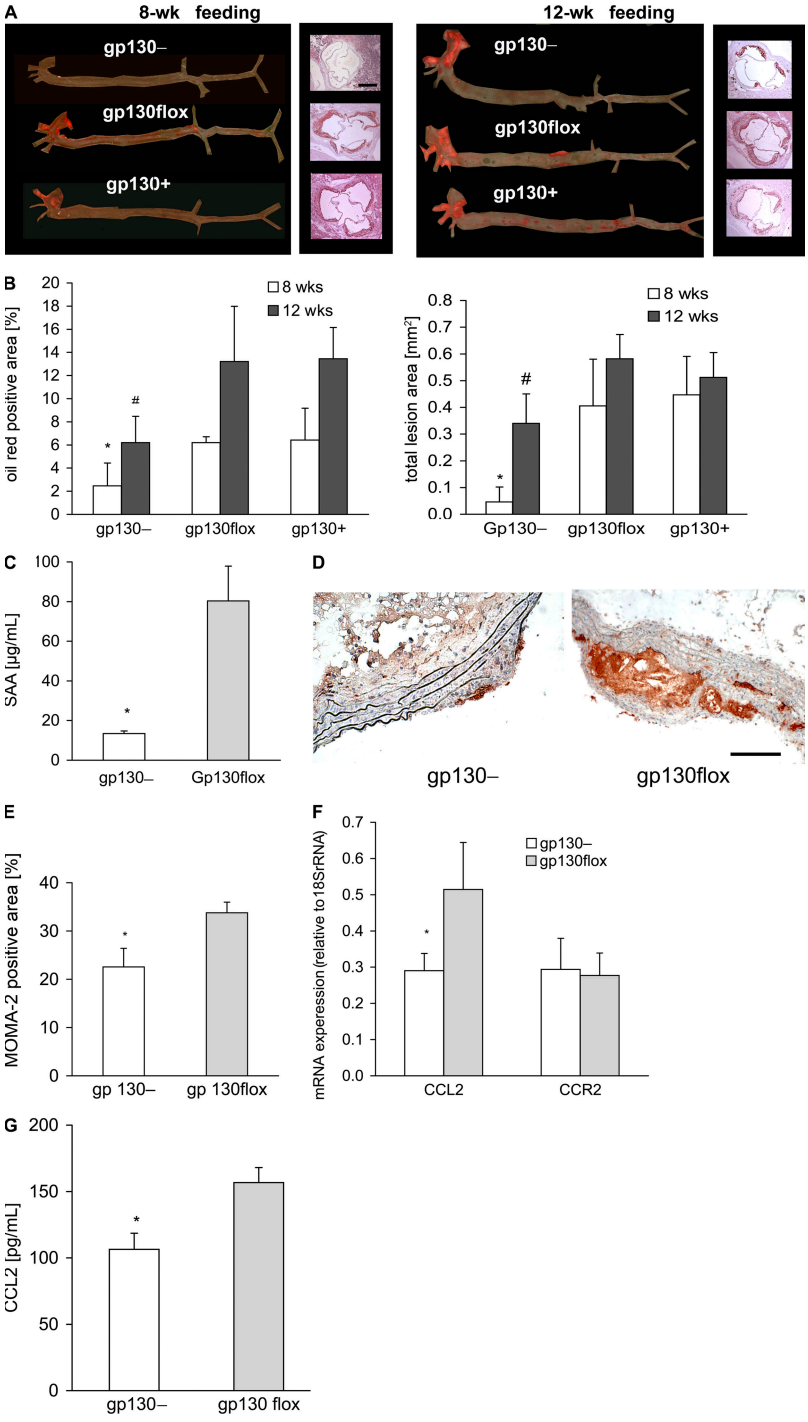

Figure 2. Analysis of atherosclerosis. Male mice were fed a Western-type diet for 8 and 12 wk. (A) representative en face preparation of aortas (left) and aortic roots (right) stained with oil red O. Red color shows lipid-laden areas representing atherosclerotic lesion coverage. Bar: (left) 1 cm; (right) 500 µm. (B) Quantification of oil red O stained areas as a percentage of whole aortic area (left) or as a total lesion area in the aortic root (right; 8-wk feeding: mean ± the SD; $n = 4$; *, $P < 0.05$ vs. gp130flox and gp130+; 12-wk feeding: mean ± the SD; $n = 4$–7; #, $P < 0.05$ vs. gp130flox and gp130+). (C) SAA concentration in plasma is significantly reduced in gp130– mice showing the lack of induction of this major hepatocyte-derived acute phase protein in response to the Western diet (mean ± the SD; $n = 7$; *, $P < 0.01$ vs. gp130flox). (D) Representative immunohistochemical staining for monocytes/macrophages (MOMA-2) demonstrates less accumulation of macrophages in the plaque areas of gp130– mice. Bar, 50 µm. (E) Quantification of MOMA-2 positively stained area as a percentage of the plaque area (mean ± the SEM; $n = 7$ animals/group with 23–43 plaques; *, $P < 0.01$ vs. gp130flox). The whole aorta was analyzed by systematic cross sectioning. (F) Semiquantitative RT-PCR of aortas after Western diet reveals reduced gene expression of CCL2 in gp130– mice, the gene responsible for monocyte attraction, whereas the expression of the corresponding receptor CCR2 is not altered (mean± the SD; $n = 7$; *, $P < 0.05$ vs. gp130flox). (G) CCL2 concentration in the plasma after Western diet is significantly reduced in gp130– mice (mean ± the SEM; $n = 7$–9; *, $P < 0.03$ vs. gp130flox).

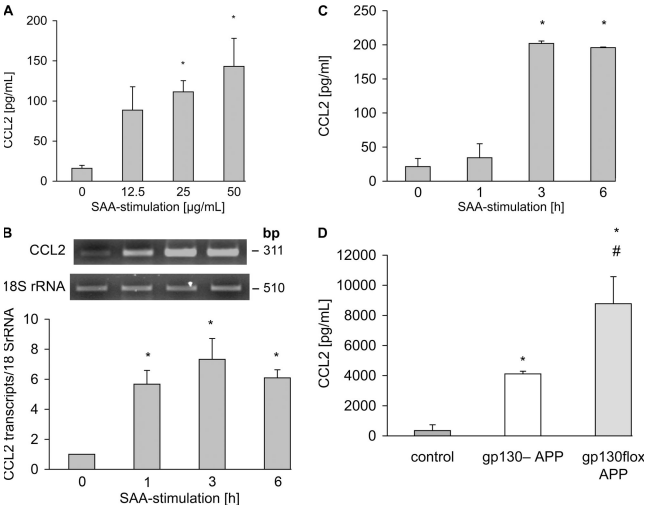

Figure 3. Stimulation experiments with mouse aortic smooth muscle cells (MASMC) isolated from wild-type mice (C57BL/6). (A) The cells were stimulated with SAA in different concentrations (12.5–50 μg/ml in DME). Measurement of CCL2 release in the supernatant was performed and shows a significant dose-dependent release of CCL2 at a SAA concentration of 25 μg/ml, which further increases at a concentration of 50 μg/ml. To exclude LPS-dependent effects derived from recombinant produced SAA, a polymyxin B assay was performed (Fig. S2). (B) Semiquantitative RT-PCR shows the time-dependent induction of CCL2 mRNA (mean ± the SEM; $n = 5$; *, $P < 0.02$ vs. 0 h). (C) Measurement of the supernatant of the same cells as in A shows the release of CCL2 (mean ± the SD; $n = 5$; *, $P < 0.01$ vs. 0 h). (D) Measurement of CCL2 concentration in the supernatants of MASMCs, demonstrating an increased release of CCL2 protein when incubated with supernatant taken from isolated gp130flox hepatocytes (mean ± the SD; $n = 5$; *, $P < 0.01$ vs. control; #, $P < 0.05$ vs. gp130–). Fig. S2 is available at http://www.jem.org/cgi/content/full/jem.20070120/DC1.

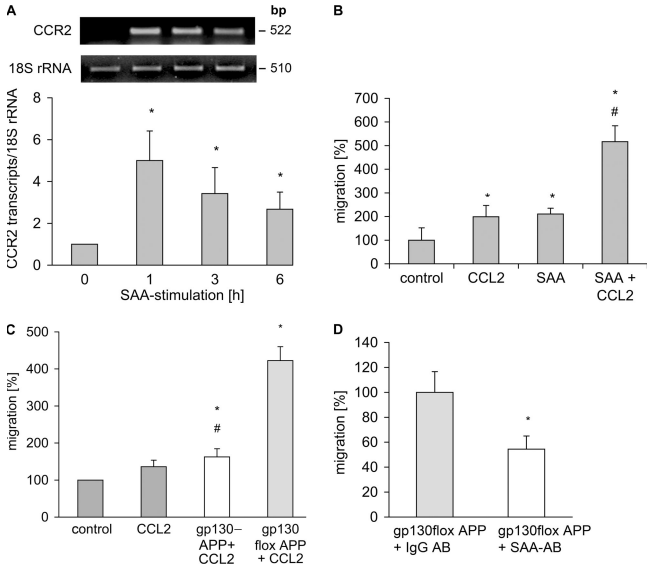

Figure 4. Stimulation and migration of macrophages upon SAA stimulation. (A) mRNA expression of the CCR2 receptor. CCR2 is upregulated as early as 1 h after stimulation with SAA (mean ± the SEM; $n = 5$; *, $P < 0.05$ vs. 0 h). (B) The migration of macrophages toward CCL2 or SAA was significantly enhanced compared with control (set to 100%) The migratory potency of macrophages to CCL2 could be still increased by preincubation of macrophages with SAA compared with the control, CCL2 or SAA alone (mean ± the SEM; $n = 5$; *, $P < 0.05$ vs. control; #, $P < 0.05$ vs. CCL2). (C) Enhanced migration of macrophages toward CCL2 after preincubation with APP containing supernatant of stimulated hepatocytes from gp130flox mice compared with supernatant from gp130– mice (mean ± the SEM; $n = 9$; *, $P < 0.05$ vs. control; #, $P < 0.05$ vs. gp130flox). (D) Reduced macrophage migration toward CCL2 after preincubation with supernatant of LIF-stimulated hepatocytes from gp130flox mice pretreated with a SAA-antibody compared with supernatant pretreated with an unspecific IgG antibody (mean ± the SEM; $n = 4$; *, $P < 0.05$ vs. IgG-pretreated supernatant).

is a member of the CC chemokine subfamily and predominantly attracts monocytes, whereas CXC family members, such as keratinocyte-derived chemokine and macrophage inflammatory protein 2, particularly induce the migration of neutrophils.

Because deletion of CCR2 in *apoE*$^{-/-}$ mice reduces atherosclerotic plaque development by decreasing macrophage recruitment to the atherosclerotic plaque (14), we next tested in a mouse macrophage cell line whether the decreased synthesis and release of APP in gp130− mice prevents cell migration. Fig. 4 A shows a strong increase in CCR2 transcripts in macrophages as early as 1 h after stimulation with SAA, whereas Fig. 4 B demonstrates enhanced migration of macrophages toward CCL2 after preincubation with SAA as a functional consequence of increased CCR2 expression. According to the cell culture experiments with MASMCs, macrophages were also stimulated with supernatant from isolated hepatocytes. Migration toward CCL2 (Fig. 4 C) was markedly enhanced when challenged with supernatant derived from gp130flox hepatocytes compared with supernatant from gp130− hepatocytes of atherosclerotic plaques.

Human genetic association of polymorphisms in the IL6ST/gp130 gene

We next examined polymorphisms in the human gp130 homologue, the IL6ST gene, in a large study sample of 513 families of Western European descent with MI. An indepth description of the patient ascertainment strategy and the clinical characteristics of the study population have been previously described (15). We tested a total of 11 single-nucleotide polymorphisms (SNPs) located in the IL6ST gene, capturing 9 SNPs located within a single 31-kb haplotype block and 2 flanking SNPs (Fig. 5, Haploview LD output), and evaluated the association with coronary artery disease (CAD) and clinical subphenotypes using the QTDT genetic analysis software packages (15). Single-point analysis identified one SNP (rs10940495) that was significantly associated with CAD before ($P < 0.05$) and after adjustment ($P < 0.01$) for age, sex, smoking, diabetes, CAD/MI, TC/high-density lipoprotein (HDL) ratio, lipid medication, and SNPs in the CRP gene that were previously associated with CRP levels (16). Two additional SNPs (rs3729960 and rs1900173) located in the

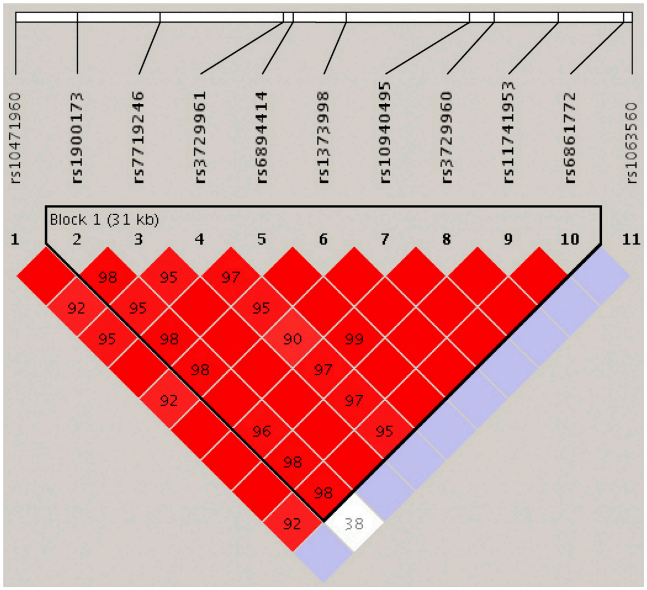

Figure 5. Haplotype diagram depicting the linkage disequilibrium structure between the SNPs in IL6ST gene. Nine SNPs fall into one block with strong linkage disequilibrium spanning 31 kb (block 1).

same haplotype block showed a trend for association with CAD. The phenotypic presentation of CAD is complex, as it relates to the location and degree of the disease. Therefore, we subsequently analyzed clinical subphenotypes of CAD, namely the atherosclerotic disease patterns as determined by angiography. To systematically characterize CAD disease burden, we previously analyzed the CAD disease pattern in families and described the heritable pattern of clinical subphenotypes, as determined by coronary angiography. We detected a particularly high heritability for the disease manifestation in the proximal part of coronary arteries, including lesions at the coronary ostium (17). When analyzing these clinical subphenotypes, a significant association ($P < 0.005$) was observed between rs1900173 and an atherosclerotic lesion at the ostium of the left or right coronary artery, as defined by the Coronary Artery Surgery Study classification (18). Additional SNPs located in the same LD block showed association to this trait at the $P < 0.05$ significance level. Table II summarizes the results of the subset and full dataset SNP analysis. Permutation testing using the algorithm implemented in QTDT determined that the association of rs1900173 with the trait "ostium" met the required global significance level, with an empirical P value of 0.0004. Even after adjustment for multiple testing using the Bonferroni correction, taking into account the haplotype structure and the number of disease segments analyzed (18 disease segments and 3 haplotype blocks), the association signal for rs1900173 remained significant ($P < 0.05$). Furthermore, we used generalized estimating equations taking into account the familial correlation of the individuals to estimate the effect of the significant associated SNP. The odds ratio (OR) for ostium stenosis for carriers of the rare allele of rs1900173 is 1.92 (95% CI, 1.03−3.6).

Table II. Significant results (P values) of association analysis in the IL6ST gene in 513 MI families using QTDT

SNP	CHD	CHD	Ostium	Ostium
	Crude analysis	Fully adjusted model	Crude analysis	Fully adjusted model
rs1063560	NS	NS	NS	NS
rs6861772	NS	NS	NS	NS
rs11741953	NS	NS	NS	NS
rs3729960	0.0882	NS	0.065	NS
rs10940495	0.0185	0.0078	NS	NS
rs1373998	NS	NS	NS	NS
rs6894414	NS	NS	0.0326	0.07
rs3729961	NS	NS	0.0201	0.043
rs7719246	NS	NS	0.0862	0.097
rs1900173	0.081	NS	0.0034	0.0023
rs10471960	NS	NS	NS	NS

The fully adjusted model includes age, gender, smoking, diabetes, BMI, CAD/MI, TC/HDL ratio, lipid medication, and three CRP gene SNPs previously associated with CRP levels.

This is consistent with a gene effect for a complex, polygenic disease. The allele frequencies of the markers are listed in Table III. Finally, we performed a haplotype-based association. A haplotype comprised of the four SNPs with positive single-point association as part of the overall haplotype block also showed a significant association (family-based association, $P < 0.05$).

To further validate our observation from the family-based approach, we investigated six haplotype-tagging SNPs in the IL6ST gene in an independent, population-based study sample from the PopGen coronary heart disease program (www.popgen.de) comprising 1,090 patients aged <55 yr with proven atherosclerosis determined by angiography. A significant association was observed between SNP rs11574780 and the trait "ostium" (crude OR 1.64, $P = 0.048$; adjusted OR 1.74,

Table III. Allele frequencies of markers

SNP rs#	MAF
	%
1063560	1
6861772	12
11741953	11
3729960	11
10940495	29
1373998	12
6894414	10
3729961	10
7719246	12
1900173	7
10471960	11
11574780	4

MAF, minor allele frequency.

P = 0.032, adjusted for age, sex, body mass index (BMI), hypertension, diabetes, TC/HDL ratio, and smoking) when comparing patients with and without ostium stenoses (>30%), thus replicating and further corroborating our initial findings.

DISCUSSION

Systemic loss of one IL-6 cytokine member exhibits mild or unexpected morphological vascular phenotypes (19), e.g., systemic deletion of IL-6 in a mouse model prone to atherosclerosis elicits detrimental effects on atherosclerotic plaque development, potentially via an IL-6–dependent downregulation of its counteracting cytokine IL-10 (20). The complete systemic gp130 knockout, in contrast, shows profound defects in cardiac and hematopoetic development, resulting in premature death in utero or soon after birth. Thus, to delineate the role of the hepatic APR in atherosclerosis, we selectively deleted the gp130 receptor in hepatocytes using the Cre-loxP system. The genetic modification was confirmed by a PCR reaction demonstrating the gene inactivation exclusively in liver, but not in heart, aorta, or spleen, and by functional analysis of gp130-dependent, LIF-induced STAT3 phosphorylation and SAA release from hepatocytes from controls, but not from gp130− mice. Thus, the introduction of loxP sites to the gp130 gene had no impact on the functionality (12) of the gp130 gene; however, Cre-mediated deletion in hepatocytes inactivates the gene and abolishes the APR.

APPs are induced by dietary cholesterol (21) and serve as markers of vascular inflammation (22). Furthermore, it could be demonstrated that SAA is deposited in murine atherosclerosis at all stages of lesion development (23), and the SAA immunoreactive area correlates highly with the lesion area, suggesting a possible role for SAA-mediated lipoprotein retention in atherosclerosis. Additionally, SAA serves as a potent chemoattractant for mouse macrophages and neutrophils (24), suggesting that SAA exerts inflammatory potencies beyond its traditional role as a marker of inflammation. Therefore, we investigated whether a high-cholesterol Western diet induces gp130-dependent SAA expression and, subsequently, atherosclerotic plaque formation. We observed significantly reduced SAA level in gp130− mice compared with gp130flox mice, which is accompanied by a reduced atherosclerotic lesion area. Collectively, these findings clearly demonstrate that the APR amplifies the development of aortic atherosclerotic lesions.

In early atherosclerotic lesions, macrophages are recruited into the vessel, take up cholesterol deposits, develop into foam cells, and form the typical lipid core (25) of the lesion. We examined the role of APR in macrophage recruitment to the vessel wall in vivo and observed a significant reduction of the macrophage-positive plaque area in gp130− mice. These findings further emphasize the impact of hepatic gp130 in particular, as it relates to the cellular components of the atherosclerotic disease process. Whether or not this process involves additional mechanisms enhanced by gp130-dependent acute phase reactants, such as the complement cascade, scavenger receptors, or NF-κB–inducing oxygen free radicals, will be further evaluated.

To confine the APP-dependent APR for macrophage migration to the aortic tissue, we determined the expression of CCL2 in isolated MASMCs, as well as CCR2 expression in mouse macrophages. Furthermore, we examined macrophage migration toward CCL2 after SAA stimulation and after stimulation with the supernatant of LIF-treated hepatocytes from gp130− and gp130flox mice. CCL2 and CCR2 expression and macrophage migration toward CCL2 are increased upon stimulation with SAA or the supernatant from hepatocytes from gp130flox mice, but significantly reduced when stimulated with supernatant from gp130− hepatocytes. These results suggest that a hepatocyte gp130-dependent APR in vivo enhances the local synthesis and release of monocyte/macrophage recruiting factors, such as CCL2 and their receptor CCR2, which stimulate macrophage migration into the vessel wall as one step in the initiation of atherosclerotic plaques. Additionally, preincubation of supernatant from LIF-stimulated gp130flox hepatocytes with a SAA antibody significantly reduced macrophage migration compared with a pretreated IgG control, pointing to SAA as the responsible APP for macrophage migration in murine atherosclerosis.

We demonstrate that SAA in mouse mediates effects similar to these observed for CRP in humans, e.g., induction of CCR2 in monocytes (26). These results are consistent with the observation that CCR2 deletion in *apoE*$^{-/-}$ mice reduces atherosclerotic plaque development by decreasing macrophage recruitment to the atherosclerotic plaque (14). In addition, the findings from the animal model further imply that gp130-dependent acute phase reactants such as SAA do not only reflect different degrees of inflammation, which has been suggested as an independent risk factor in a variety of cardiovascular diseases. These observations are consistent with the notion that gp130-dependent acute phase reactants, such as SAA, are direct mediators for plaque formation in murine atherosclerosis.

Given the known differences between the mouse model and humans related to the inflammatory response, as well as disease mechanisms, and after the functional results from our animal model, the question arises whether gp130 also plays a significant role in human atherosclerosis. Comparative genetics methods offer a successful strategy for the translation of findings from rodent disease models, i.e., inbred strains, transgenic, or knockout models, to clinically relevant settings by identifying homologous genes in the human genome for genetic association studies (27, 28). Therefore, we tested in two independent populations whether genetic variation in the human homologue of gp130, i.e., IL6ST, influences phenotypes of atherosclerosis. We obtained significant evidence for an association of SNPs in the human homologue IL6ST gene and atherosclerotic disease in humans for CAD as a phenotype in a large set of families. Although the direct mechanism of action for the identified SNPs remains to be determined in future experiments, the results from our animal models in conjunction with the association data suggests an activating effect.

More importantly, we also detected a highly significant association for a stenosis of the ostium of the coronary arteries. The association with an atherosclerotic lesion at the ostium is

of particular clinical relevance because occlusion of the ostium or proximal segment of a coronary artery (i.e., the left anterior descending artery) results in a substantial reduction of blood flow to large parts of the left ventricle.

Consequently, occlusion of the ostium or the left anterior descending artery is often considered the morphological correlate of sudden cardiac death or MI with a particularly high mortality. To further evaluate the robustness of this strong association signal in families, we could replicate the association signal for an ostium stenosis in a second independent population-based cohort. In light of the functional evidence from the animal model, the replicated association in humans that remained significant after adjusting for multiple testing, together with a haplotype-based analysis, provides strong evidence that gp130 also plays an important role in human disease. Our findings might therefore guide toward an improved risk assessment in patients with mutations in the gp130 gene and an increased risk of CAD.

In summary, we demonstrated that a gp130-driven acute phase reaction is a critical regulator for the process of atherosclerotic plaque development. Our observations strengthen the utility of comparative genetics approaches for the identification of susceptibility genes for common, complex diseases in humans, and thus allow a direct translation of experimental results into clinical relevance.

MATERIALS AND METHODS

Mice

Mice with a floxed gp130 gene (*gp130*$^{flox/flox}$) and mice with the albumin-specific transgene for Cre-recombinase (*alb-cre*^{tg}) were crossed with apolipoprotein E–deficient mice (*apoE*$^{-/-}$; Charles River Laboratories) to obtain mice lacking gp130 specifically within hepatocyte (*alb-cre*^{tg}*;gp130*$^{flox/flox}$*;apoE*$^{-/-}$). Littermates with floxed gp130 (*gp130*$^{flox/flox}$*;apoE*$^{-/-}$) and the wild-type allele (*gp130*$^{+/+}$*;apoE*$^{-/-}$) served as controls. All animals were backcrossed for 10 generations on a C57BL/6 genetic background, kept under specific pathogen-free conditions in the animal facility at the Medizinische Hochschule Hannover (Hannover, Germany). All experiments were approved by the governmental animal ethics committee and performed according to the guidelines of the Federation of European Animal Science Associations. At 10 wk of age, male mice were subjected to Western-type dieting (20% fat, 0.1% cholesterol, and Altromin) for 8 and 12 wk.

Genotyping

All mice were genotyped by PCR using previously described primer sequences (29), and deletion at the exon 16 locus of the gp130 gene was verified as recently reported (13).

Cell culture

Hepatocytes were isolated (30), 10^6 cells were cultured on 6-cm culture plates (Nunc) with DME (Invitrogen) containing 4.5 g/L glucose, 10% FCS, and penicillin/streptomycin for 24 h. Cells were stimulated with 50 ng/ml LIF (Chemicon) for 0–6 h. MASMCs were isolated as described previously (31) and maintained in DME (1.5 g/liter glucose; Biochrom). Under serum-free conditions, cells were stimulated either with 12.5, 25, or 50 μg/ml SAA (Peprotech) or with supernatant of hepatocytes diluted 1:2 in DME for the indicated times. Macrophages (MH-S murine alveolar macrophage cell line; LGC Promochem) were cultivated in nonadherent suspension culture with RPMI 1640 (Invitrogen) containing 10% FCS, penicillin/streptomycin, and 3.5 μl/liter β-mercaptoethanol. Cells were stimulated under serum deprivation (1% FCS) for the indicated times.

Migration experiment

10^5 serum-starved murine macrophages (MHS cells) were used per well (Corning Transwell) to measure migration over a period of 24 h through an 8-μm pore size membrane in response to 50 ng/ml murine CCL2 (Biosource), 25 μg/ml SAA with previous stimulation with or without 25 μg/ml SAA, supernatant from LIF-stimulated hepatocytes for 1 h, or supernatant from LIF-stimulated hepatocytes pretreated either with a goat anti–mouse SAA antibody (10 μg/10 μl for 1 h; R&D Systems) or with an unspecific goat anti–mouse IgG (10 μg/10 μl for 1 h; Sigma-Aldrich).

Protein cytokine array

A protein cytokine array kit was purchased from RayBiotech. In brief, the membranes were blocked with a blocking buffer, and then 1 ml of medium from either unstimulated or SAA-stimulated (25 μg/ml for 3 h) SMC was added and incubated at room temperature for 2 h. The membranes were washed, and 1 ml of primary biotin-conjugated antibody was added and incubated at room temperature for 2 h. The membranes were incubated with 2 ml of horseradish peroxidase–conjugated streptavidin at room temperature for 30 min. The membranes were developed by using enhanced chemiluminescence-type solution, exposed to film, and processed by autoradiography.

Western blot

30-μg protein extracts were separated by denaturing 10% SDS-PAGE and transferred to PVDF membrane (GE Healthcare). Proteins were probed with a rabbit anti–mouse p-STAT-3 antibody (Cell Signaling Technology) and visualized by secondary anti–rabbit-HRP antibody (GE Healthcare) and ECL solution. Equal protein loading was verified by reprobing the membrane with rabbit anti–mouse STAT-3 (Santa Cruz Biotechnology). STAT3 phosphorylation was quantified relative to total STAT3 expression using GelDoc image analysis system (Bio-Rad Laboratories).

Tissue preparation

For the analysis of atherosclerotic lesion areas, aortas were prepared en face, as previously described (20). Within the aortic root, lesion areas were analyzed in cross sections obtained at the level of all three leaflets of the aortic valve. To assess cellular morphology, cross sections were stained with hematoxylin and eosin. The lesion areas in the aortic root were determined via computer-assisted image quantification (Axio Vision; Carl Zeiss MicroImaging, Inc.) (32). For immunohistochemistry, the aorta was isolated, embedded in OCT, divided into four sections, and cut systematically every 60 μm in 6-μm cross sections with plaques to obtain serial sections throughout the vessel (20). Monocytes/macrophages were detected with rat anti–mouse MOMA-2 antibody (Acris), followed by rabbit mouse-absorbed anti–rat antibody-HRP (Vector Laboratories) using AEC+ substrate chromogen (DakoCytomation). Morphometric data were obtained by image analysis (QWin software; Leica; Axiovert 200M; Carl Zeiss MicroImaging, Inc.).

Plasma analyses

Plasma samples were collected after an overnight fast. TC and triglycerides were determined by colorimetric assays (WAKO Chemicals) after the separation of lipoprotein subfractions by ultracentrifugation (20, 33). CCL2 (R&R System) and SAA (Tridelta) were measured by ELISA.

Semiquantitative RT-PCR

Gene expression was assessed by semiquantitative RT-PCR. Total RNA was isolated using TriFast-Reagent (peqLAB), and reverse transcribed (Superscript reverse transcriptase; Invitrogen) with oligo(dT) primers. The RT products were amplified using *Taq* DNA polymerase (Invitrogen, Biometra cycler). PCR was performed for 18 cycles (18S rRNA), for 34 cycles (CCL2), and for 40 cycles (CCR2), using oligonucleotides obtained from MWG Biotech. PCR products were separated on 1% Agarose gels and quantified relative to 18S rRNA expression using the GelDoc image analysis system (Bio-Rad Laboratories).

Statistical analysis

Data are presented as the means ± the SD or the SEM, as indicated. Comparisons between groups were performed by Student's *t* test assuming two-tailed distribution and unequal variances.

Study population

All study participants gave written informed consent, and the study was approved by the ethics committees at the Medical College of Wisconsin (Milwaukee, WI), the University of Regensburg (Regensburg, Germany), and the University of Kiel (Kiel, Germany).

Subject ascertainment and phenotyping

MI/CAD. An indepth description of the patient ascertainment strategy and the clinical characteristics of the study population have been previously reported for MI families (15). In brief, Western European families were included in the study if probands had suffered a MI (as documented by criteria chosen according to the published definitions of the Monitoring of Trends and Determinants in Cardiovascular Disease investigators of the World Health Organization) before the age of 60 and affected siblings had a MI or underwent percutaneous transluminal coronary angioplasty or coronary artery bypass grafting. Subphenotypes of CAD were collected from coronary angiographies. A detailed description of the phenotypes, the phenotyping protocol, and a heritability analysis has been previously published (17). In brief, coronary arteries were divided into 16 subsegments. Qualitative phenotypes were used for family-based association analysis.

The PopGen (www.popgen.de) coronary heart disease program scrutinized the records from all patients in Northern Schleswig-Holstein who underwent cardiac catheterization between January 1, 1997 and June 30, 2003. Because of the geographic characteristics of the region, this represents the entire disease population, which is diagnosed at only six coronary care centers. 1,607 patients <55 yr old with diagnosis of atherosclerosis through cardiac catheter were contacted, and 1,090 patient DNA samples (M 921–83.6%) with corresponding clinical datasets were available for the study. Catheter reports were evaluated and catheter films rescored if necessary. A full set of clinical and laboratory data was extracted from patient files.

SNP identification and genotyping

Based on the available SNP and linkage disequilibrium data from public databases, we selected 11 SNPs covering the whole gene, as well as the 5′- and 3′-regions. Only SNPs with a minor allele frequency ≥5% for the IL6ST gene and flanking SNP were selected. Genotyping of SNPs rs1063560, rs6861772, rs11741953, rs3729960, rs10940495, rs1373998, rs6894414, rs3729961, rs7719246, rs1900173, and rs10471960 was performed at the Medical College of Wisconsin using TaqMan technology (Applied Biosystems). For genotyping the PopGen samples, 6 SNPs (rs7719246, rs11574780, rs10940495, rs6870870, rs10471960, and rs1900173) were genotyped at the University of Kiel using SNPlex technology (Applied Biosystems).

Statistical analysis

Linkage disequilibrium estimation. The analysis program Haploview (version 3.2) was used to calculate and visualize linkage disequilibrium and haplotype-block patterns of the genotyped SNPs (34).

Association analysis. The QTDT program was used for the quantitative family-based single SNP association analysis and permutation testing (35). P values for single SNP association analysis were adjusted for age, gender, BMI, presence or absence of diabetes, smoking status, presence or absence of CAD/MI, lipid medication, and TC/HDL ratio. Empirical P values were calculated using a permutation procedure with 10,000 permutations, as implemented in QTDT. Haplotypes were calculated using the Genehunter 2.1 software package. Genotypic odds ratios in the MI families were calculated using generalized estimation equations taking into account the correlation of the individuals (PROC GENMOD, SAS V9). Association analysis in the PopGen study sample was performed using logistic regression analysis as implemented in SPSS 12.0. P values were adjusted for age, gender, BMI, presence or absence of diabetes, smoking status, and TC/HDL ratio. Before the analysis, all SNPs were evaluated for deviation from Hardy-Weinberg-Equilibrium by χ^2 statistics.

Online supplemental material

Fig. S1 shows mouse cytokines that are up-regulated and released from MASMC stimulated with SAA. Fig. S2 shows that the SAA-induced CCR2 release from MASMC is not mediated by LPS. The online version of this article is available at http://www.jem.org/cgi/content/full/jem.20070120/DC1.

The authors gratefully acknowledge the excellent technical support of Tanja Sander, Silke Pretzer, Lena Bossen, and Tanja Wesse. We thank Dr. Alexander Reinecke for phenotype scoring, Dr. Arne Schäfer for data handling and quality management, and Rainer Vogler for documentation of the PopGen sample. Finally, we thank the physicians at the Departments of Cardiology/Cardiac Surgery at university hospital Schleswig-Holstein, regional hospitals of Rensburg, Flensburg (Diakonissenanstalt), Heide (Westküstenklinikum), Schleswig (Mathin-Luther-Hospital), and the private cardiac center of Drs. Thümmel and Hinrichsen.

H. Drexler, B. Schieffer, C. Trautwein, and H. Schunkert are supported by funding from the Deutsche Forschungsgemeinschaft (Sonderforschungsbereich 566 [H. Drexler and B. Schieffer]; Sonderforschungsbereich 542 [C. Trautwein]; and Schu672/10-1, Schu672/12-1, Schu672/14-1 [H. Schunkert]). H. Drexler is a recipient of a Leducq Grant. U.J.F. Tietge is supported by the Netherlands Organization for Scientific Research (NWO, VIDI grant 917-56-358). U. Bavendiek is supported in part by funds from National Heart, Lung, and Blood Institute (R01-HL074321). S. Schreiber is supported by grants from the Bundesministerium für Bildung und Forschung (01GR0412, 01GR0468, and 01GS0426).

The authors declare that they have no competing financial interests.

Submitted: 16 January 2007
Accepted: 19 June 2007

REFERENCES

1. Ross, R. 1999. Atherosclerosis - an inflammatory disease. *N. Engl. J. Med.* 340:115–126.
2. Huber, S.A., P. Sakkinen, D. Conze, N. Hardin, and R. Tracy. 1999. Interleukin-6 exacerbates early atherosclerosis in mice. *Arterioscler. Thromb. Vasc. Biol.* 19:2364–2367.
3. Elhage, R., S. Clamens, S. Besnard, Z. Mallat, A. Tedgui, J.-F. Arnal, A. Maret, and F. Bayard. 2001. Involvement of interleukin-6 in atherosclerosis but not in the prevention of fatty streak formation by 17β-estradiol in apolipoprotein E-deficient mice. *Atherosclerosis.* 156:315–320.
4. Ridker, P.M., C.H. Hennekens, J.E. Buring, and N. Rifai. 2000. C-reactive protein and other markers of inflammation in the prediction of cardiovascular disease in women. *N. Engl. J. Med.* 342:836–843.
5. Paoletti, R., A.M. Gotto Jr., and D.P. Hajjar. 2004. Inflammation in atherosclerosis and implications for therapy. *Circulation.* 109:III20–III26.
6. Fukada, T., M. Hibi, Y. Yamanaka, M. Takahashi-Tezuka, Y. Fujitani, T. Yamaguchi, K. Nakajima, and T. Hirano. 1996. Two signals are necessary for cell proliferation induced by a cytokine receptor gp130: involvement of STAT3 in anti-apoptosis. *Immunity.* 5:449–460.
7. Heinrich, P.C., I. Behrmann, G. Müller-Newen, F. Schaper, and L. Graeve. 1998. Interleukin-6-type cytokine signalling through the gp130/Jak/STAT pathway. *Biochem. J.* 334:297–314.
8. Schaper, F., C. Gendo, M. Eck, J. Schmitz, C. Grimm, D. Anhuf, I.M. Kerr, and P.C. Heinrich. 1998. Activation of the protein tyrosine phosphatase SHP2 via the interleukin-6 signal transducing receptor protein gp130 requires tyrosine kinase Jak1 and limits acute-phase protein expression. *Biochem. J.* 335:557–565.
9. Ku, N.O., and R.F. Mortensen. 1993. The mouse C-reactive protein (CRP) gene is expressed in response to IL-1 but not IL-6. *Cytokine.* 5:319–326.
10. Uhlar, C.M., and A.S. Whitehead. 1999. Serum amyloid A, the major vertebrate acute-phase reactant. *Eur. J. Biochem.* 265:501–523.
11. Kellendonk, C., C. Opherk, K. Anlag, G. Schütz, and F. Tronche. 2000. Hepatocyte-specific expression of cre recombinase. *Genesis.* 26:151–153.

12. Betz, U.A.K., W. Bloch, M. van den Broek, K. Yoshida, T. Taga, T. Kishimoto, K. Addicks, K. Rajewsky, and W. Müller. 1998. Postnatally induced inactivation of gp130 in mice results in neurological, cardiac, hematopoietic, immunological, hepatic, and pulmonary defects. *J. Exp. Med.* 188:1955–1965.
13. Streetz, K.L., T. Wuestefeld, C. Klein, K.-J. Kallen, F. Tronche, U.A.K. Betz, G. Schütz, M.P. Manns, W. Müller, and C. Trautwein. 2003. Lack of gp130 expression in hepatocytes promotes liver injury. *Gastroenterology.* 125:532–543.
14. Boring, L., J. Gosling, M. Cleary, and I.F. Charo. 1998. Decreased lesion formation in CCR2−/− mice reveals a role for chemokines in the initiation of atherosclerosis. *Nat. Med.* 394:894–897.
15. Broeckel, U., C. Hengstenberg, B. Mayer, S. Holmer, L.J. Martin, A.G. Comuzzie, J. Blangero, P. Nurnberg, A. Reis, G.A. Riegger, et al. 2002. A comprehensive linkage analysis for myocardial infarction and its related risk factors. *Nat. Genet.* 30:210–214.
16. Carlson, C.S., M.A. Eberle, M.J. Rieder, J.D. Smith, L. Kruglyak, and D.A. Nickerson. 2003. Additional SNPs and linkage-disequilibrium analyses are necessary for whole-genome association studies in humans. *Nat. Genet.* 33:518–521.
17. Fischer, M., U. Broeckel, S. Holmer, A. Baessler, C. Hengstenberg, B. Mayer, J. Erdmann, G. Klein, G. Riegger, H.J. Jacob, and H. Schunkert. 2005. Distinct heritable patterns of angiographic coronary artery disease in families with myocardial infarction. *Circulation.* 111:855–862.
18. Ringqvist, I., L.D. Fisher, M. Mock, K.B. Davis, H. Wedel, B.R. Chaitman, E. Passamani, R.O. Russell Jr., E.L. Alderman, N.T. Kouchoukas, et al. 1983. Prognostic value of angiographic indices of coronary artery disease from the Coronary Artery Surgery Study (CASS). *J. Clin. Invest.* 71:1854–1866.
19. Kopf, M., H. Baumann, G. Freer, M. Freudenberg, M. Lamers, T. Kishimoto, R. Zinkernagel, H. Bluethmann, and G. Kohler. 1994. Impaired immune and acute-phase responses in interleukin-6-deficient mice. *Nature.* 368:339–342.
20. Schieffer, B., T. Selle, A. Hilfiker, D. Hilfiker-Kleiner, K. Grote, U.J. Tietge, C. Trautwein, M. Luchtefeld, C. Schmittkamp, S. Heeneman, et al. 2004. Impact of interleukin-6 on plaque development and morphology in experimental atherosclerosis. *Circulation.* 110:3493–3500.
21. Lewis, K.E., E.A. Kirk, T.O. McDonald, S. Wang, T.N. Wight, K.D. O'Brien, and A. Chait. 2004. Increase in serum amyloid a evoked by dietary cholesterol is associated with increased atherosclerosis in mice. *Circulation.* 110:540–545.
22. Pasceri, V., J.S. Cheng, J.T. Willerson, and E.T. Yeh. 2001. Modulation of C-reactive protein-mediated monocyte chemoattractant protein-1 induction in human endothelial cells by anti-atherosclerosis drugs. *Circulation.* 103:2531–2534.
23. O'Brien, K.D., T.O. McDonald, V. Kunjathoor, K. Eng, E.A. Knopp, K. Lewis, R. Lopez, E.A. Kirk, A. Chait, T.N. Wight, et al. 2005. Serum amyloid A and lipoprotein retention in murine models of atherosclerosis. *Arterioscler. Thromb. Vasc. Biol.* 25:785–790.
24. Badolato, R., J.M. Wang, W.J. Murphy, A.R. Lloyd, D.F. Michiel, L.L. Bausserman, D.J. Kelvin, and J.J. Oppenheim. 1994. Serum amyloid A is a chemoattractant: induction of migration, adhesion, and tissue infiltration of monocytes and polymorphonuclear leukocytes. *J. Exp. Med.* 180:203–209.
25. Libby, P. 2002. Inflammation in atherosclerosis. *Nature.* 420:868–874.
26. Han, K.H., K.-H. Hong, J.-H. Park, J. Ko, D.-H. Kang, K.-J. Choi, M.-K. Hong, S.-W. Park, and S.-J. Park. 2004. C-reactive protein promotes monocyte chemoattractant protein-1–mediated chemotaxis through upregulating CC chemokine receptor 2 expression in human monocytes. *Circulation.* 109:2566–2571.
27. Wang, X., M. Ria, P.M. Kelmenson, P. Eriksson, D.C. Higgins, A. Samnegard, C. Petros, J. Rollins, A.M. Bennet, B. Wiman, et al. 2005. Positional identification of TNFSF4, encoding OX40 ligand, as a gene that influences atherosclerosis susceptibility. *Nat. Genet.* 37:365–372.
28. Wang, X., N. Ishimori, R. Korstanje, J. Rollins, and B. Paigen. 2005. Identifying novel genes for atherosclerosis through mouse-human comparative genetics. *Am. J. Hum. Genet.* 77:1–15.
29. Betz, U.A., C.A. Vosshenrich, K. Rajewsky, and W. Müller. 1996. Bypass of lethality with mosaic mice generated by Cre-loxP-mediated recombination. *Curr. Biol.* 6:1307–1316.
30. Swift, L.L., M.H. Farkas, A.S. Major, K. Valyi-Nagy, M.F. Linton, and S. Fazio. 2001. A recycling pathway for resecretion of internalized apolipoprotein E in liver cells. *J. Biol. Chem.* 276:22965–22970.
31. Grote, K., I. Flach, M. Luchtefeld, E. Akin, S.M. Holland, H. Drexler, and B. Schieffer. 2003. Mechanical stretch enhances mRNA expression and proenzyme release of matrix metalloproteinase-2 (MMP-2) via NAD(P)H oxidase-derived reactive oxygen species. *Circ. Res.* 92:e80–e86.
32. Bavendiek, U., A. Zirlik, S. LaClair, L. MacFarlane, P. Libby, and U. Schonbeck. 2005. Atherogenesis in mice does not require CD40 ligand from bone marrow-derived cells. *Arterioscler. Thromb. Vasc. Biol.* 25:1244–1249.
33. Tietge, U.J., C. Maugeais, W. Cain, D. Grass, J.M. Glick, F.C. de Beer, and D.J. Rader. 2000. Overexpression of secretory phospholipase A(2) causes rapid catabolism and altered tissue uptake of high density lipoprotein cholesteryl ester and apolipoprotein A-I. *J. Biol. Chem.* 275:10077–10084.
34. Aiello, R.J., P.-A.K. Bourassa, S. Lindsey, W. Weng, E. Natoli, B.J. Rollins, and P.M. Milos. 1999. Monocyte chemoattractant protein-1 accelerates atherosclerosis in apolipoprotein E-deficient mice. *Arterioscler. Thromb. Vasc. Biol.* 19:1518–1525.
35. Abecasis, G.R., L.R. Cardon, and W.O. Cookson. 2000. A general test of association for quantitative traits in nuclear families. *Am. J. Hum. Genet.* 66:279–292.